Redox Biology 9 (2016) 229–243

Contents lists available at ScienceDirect

Redox Biology

journal homepage: www.elsevier.com/locate/redox

Research Paper

The deleterious effect of cholesterol and protection by quercetin on mitochondrial bioenergetics of pancreatic β-cells, glycemic control and inflammation: *In vitro* and *in vivo* studies

Catalina Carrasco-Pozo [a,b,*], Kah Ni Tan [b], Marjorie Reyes-Farias [a], Nicole De La Jara [a], Shyuan Thieu Ngo [b,c], Diego Fernando Garcia-Diaz [a], Paola Llanos [d], Maria Jose Cires [a], Karin Borges [b]

[a] Department of Nutrition, Faculty of Medicine, University of Chile, P.O. Box 8380453, Santiago, Chile
[b] School of Biomedical Sciences, The University of Queensland, Brisbane QLD 4072, Australia
[c] The University of Queensland Centre for Clinical Research, Brisbane QLD 4006, Australia
[d] Institute for Research in Dental Sciences, Faculty of Dentistry, University of Chile, Santiago, Chile

ARTICLE INFO

Article history:
Received 2 July 2016
Received in revised form
22 July 2016
Accepted 18 August 2016
Available online 26 August 2016

Keywords:
Cholesterol
Glycemic control
Mitochondrial dysfunction
Quercetin
Sirtuin-1
NFκB

ABSTRACT

Studying rats fed high cholesterol diet and a pancreatic β-cell line (Min6), we aimed to determine the mechanisms by which quercetin protects against cholesterol-induced pancreatic β-cell dysfunction and impairments in glycemic control. Quercetin prevented the increase in total plasma cholesterol, but only partially prevented the high cholesterol diet-induced alterations in lipid profile. Quercetin prevented cholesterol-induced decreases in pancreatic ATP levels and mitochondrial bioenergetic dysfunction in Min6 cells, including decreases in mitochondrial membrane potentials and coupling efficiency in the mitochondrial respiration (basal and maximal oxygen consumption rate (OCR), ATP-linked OCR and reserve capacity). Quercetin protected against cholesterol-induced apoptosis of Min6 cells by inhibiting caspase-3 and -9 activation and cytochrome c release. Quercetin prevented the cholesterol-induced decrease in antioxidant defence enzymes from pancreas (cytosolic and mitochondrial homogenates) and Min6 cells and the cholesterol-induced increase of cellular and mitochondrial oxidative status and lipid peroxidation. Quercetin counteracted the cholesterol-induced activation of the NFκB pathway in the pancreas and Min6 cells, normalizing the expression of pro-inflammatory cytokines. Quercetin inhibited the cholesterol-induced decrease in *sirtuin 1* expression in the pancreas and pancreatic β-cells. Taken together, the anti-apoptotic, antioxidant and anti-inflammatory properties of quercetin, and its ability to protect and improve mitochondrial bioenergetic function are likely to contribute to its protective action against cholesterol-induced pancreatic β-cell dysfunction, thereby preserving glucose-stimulated insulin secretion (GSIS) and glycemic control. Specifically, the improvement of ATP-linked OCR and the reserve capacity are important mechanisms for protection of quercetin. In addition, the inhibition of the NFκB pathway is an important mechanism for the protection of quercetin against cytokine mediated cholesterol-induced glycemic control impairment. In summary, our data highlight cellular, molecular and bioenergetic mechanisms underlying quercetin's protective effects on β-cells *in vitro* and *in vivo*, and provide a scientifically tested foundation upon which quercetin can be developed as a nutraceutical to preserve β-cell function.

1. Introduction

Cholesterol plays an important role in pancreatic β-cell dysfunction. Mice with specific inactivation of ABCA1 (ATP-binding cassette transporter subfamily A member 1), a transporter that mediates reverse cholesterol efflux show impaired glucose tolerance and insulin secretion [1,2]. Moreover, a direct link has been found between elevated cholesterol and reduced insulin secretion in islets isolated from C57BL/6J mice and in INS-1 rat pancreatic β-cells [3], as well as in Min6 cells [4], whereby insulin secretion can be normalized through cholesterol depletion [3]. LDL receptor deficient mice exhibit hypercholesterolemia with elevated cholesterol levels in pancreatic islets, which is associated with β-cell

* Corresponding author at: Department of Nutrition, Faculty of Medicine, University of Chile, P.O. Box 8380453, Santiago, Chile.
E-mail address: catalinacarrasco@med.uchile.cl (C. Carrasco-Pozo).

http://dx.doi.org/10.1016/j.redox.2016.08.007

dysfunction, impaired glucose tolerance and reduced glucose-stimulated insulin secretion (GSIS) [5]. Given that pancreatic β-cells are considered to be particularly susceptible to oxidative stress due to their relatively low antioxidant enzyme content [6], it has been suggested that cholesterol may induce β-cell dysfunction by promoting apoptosis through oxidative stress pathways [4,7] and mitochondrial damage [4,8] and also by altering membrane fluidity [9]. Although the molecular mechanism underlying cholesterol-induced inflammatory damage to β-cells is not well understood, it has been shown that cholesterol is able to increase TNF-α (tumor necrosis factor alpha), interleukin-6 (IL-6) and macrophage colony-stimulating factor (*m*-CSF) in macrophages [10], which could contribute to the damage of β-cells.

Quercetin (QUE) is a natural polyphenolic flavonoid which is believed to have widespread health benefits due to a combination of its properties. Quercetin can be (a) antioxidant, by free radical scavenging and induction of antioxidant defence via nuclear factor (erythroid-derived 2)-like 2 (Nrf2) activation, (b) anti-inflammatory through reducing pro- and increasing anti-inflammatory cytokines *via* nuclear factor kappa B (NFκB) inactivation and (c) anti-apoptotic by modulating JNK (c-Jun N-terminal kinase) and ERK (extracellular-signal-regulated kinase)-pathways [11–14]. Recent *in vitro* evidence showed the mitochondrial protective effect of QUE, restoring mitochondrial membrane potential (MMP), ATP levels and complex-I activity altered by indomethacin, a non-steroidal anti-inflammatory drug, in intestinal Caco-2 cells [15]. Interestingly, compared to other polyphenols like resveratrol, rutin and epigallocatechin gallate, QUE was the most efficient in protecting against mitochondrial dysfunction [15]; this could be due to its ability to enter cells and accumulate in mitochondria [15,16]. In addition, it has been shown that QUE up-regulates mitochondrial complex-I activity to protect against programmed cell death in rotenone model of Parkinson's disease in rats [17]. Quercetin also has been shown to increase markers of mitochondrial biogenesis, such as expression of *sirtuin 1* (*Sirt1*), a nicotinamide adenosine dinucleotide-dependent histone deacetylase, and peroxisome proliferator-activated receptor gamma coactivator-1-alpha (*PGC-1α*), in soleus muscle and brain; these changes were associated with an improvement in exercise performance [18].

Cytokine-induced pancreatic β-cell apoptosis is considered the main mechanism for β-cell death [19]. Cytokine-induced mitochondrial dysfunction through activation of the NFκB-pathway and oxidative stress may also trigger β-cell death [20–23]. Quercetin has been shown to prevent cytokine-induced pancreatic β-cell death by counteracting the mitochondrial apoptosis pathway and NFκB signalling, thereby preserving glucose-stimulated insulin secretion (GSIS) [20–23]. In addition, QUE *via* the ERK1/2 pathway, protects β-cells against oxidative damage [24]. Overexpression of *Sirt1* in β-cells improves GSIS, while *Sirt1* knockdown results in impaired response to glucose [25]. Given that impaired GSIS is a hallmark of the transition from the pre-diabetic to diabetic state [26], QUE has been proposed to be a promising anti-diabetic agent due to its ability to induce antioxidant effects through Sirt1. Also, QUE is known to protect β-cells against damage and to ameliorate hyperglycemia in diabetic animals by reducing oxidative stress, preserving β-cell mass, and lowering plasma glucose and cholesterol levels [27,28]. Based on evidence that QUE accumulates in mitochondria [15,16], its β-cell protective effects may rely not only in its anti-inflammatory and anti-oxidant properties, but also on its protection of mitochondrial function. The present study aimed to determine the mechanism underlying the protective effect of QUE on the impairment of GSIS in a pancreatic β-cell line exposed to cholesterol and glycemic control in rats fed a high-cholesterol diet. This study addresses the protective effects of QUE on mitochondrial bioenergetic dysfunction, inflammation, oxidative stress and apoptosis induced by high levels of cholesterol.

2. Materials and methods

2.1. Animals and diets

The study protocol was approved by the Animal Ethics Committee of the Faculty of Medicine of the University of Chile (Approval No. CBA# 0586 FMUCH) and all procedures were performed in compliance with the Guidelines for Care and Use of Laboratory Animals at the Faculty of Medicine. Male Wistar rats (90–110 g, 5–6 weeks old) from the Faculty of Medicine were housed in a 12 h light/dark schedule at room temperature with water *ad libitum*. Forty animals were randomly distributed into 5 groups and fed standard diet (AIN-76A/Clinton-Cybulsky Cholesterol Series #1-107); standard diet supplemented with quercetin (0.5% w/w); high-cholesterol (HC) diet (1.25% cholesterol w/w, AIN-76A/Clinton-Cybulsky Cholesterol Series #3-107); or HC diet supplemented with either quercetin (0.5% w/w) or ezetimibe (0.001% w/w) for 4 weeks (N=8 rats per group). Ezetimibe blocks Niemann-Pick C1 Like 1 (NPC1L1) protein in the small intestine, a transporter that mediates cholesterol absorption [29].

2.2. Laboratory determinations and sample collection

Tail blood glucose levels were determined after 12 h-fasted (from 9 pm) animals after 2 and 4 weeks of treatment using an Accu-chek glucometer (Roche, Mannheim, Germany). Immediately afterwards in 4 week treated rats a glucose tolerance test (IPGTT, 2 g/kg.i.p.) was assayed and blood glucose levels were determined from tail bleeds. Twenty four h after the IPGTT, plasma glucose and insulin levels were measured using a colorimetric kit and a rat insulin ELISA kit, respectively. Cholesterol levels were determined using a colorimetric colestat enzimática AA kit and pro-inflammatory cytokines using a magnetic bead Multiplex assay on plasma obtained from the inferior vena cava under ketamine:xylazine anaesthesia (100 mg/kg:10 mg/kg, i.p.). Lipid profile (LDL, VLDL and HDL) was performed by Laboratorio Clinico Medicina Nuclear (Santiago, Chile). Pancreases were removed and stored in 4% paraformaldehyde and embedded in paraffin for immunohistochemistry. Pancreatic tissue from the same rats was also stored in RNA later (Thermo Scientific, MA USA) for gene expression assays and at −80 °C for biochemical analyses, including the quantification of cholesterol using the Amplex® Red Cholesterol Assay Kit (Thermo Scientific, MA USA).

2.3. Cell culture

Min6 cells (p38–p51) were cultured in DMEM (25 mM glucose) supplemented with 10% heat-inactivated FBS, 100 IU/ml penicillin and 100 μg/ml streptomycin. All experiments were conducted in unsupplemented DMEM media. A “water-soluble cholesterol” containing 47 mg of cholesterol/g solid (molar ratio, 1:6 cholesterol/ methyl-β-cyclodextrin, Sigma, MO, USA) was used to deliver cholesterol to the cells [4,8,30,31]. Considering that 5 mM methyl-β-cyclodextrin depletes cholesterol from membranes [30,32], a ten-time lower concentration was used.

2.4. Insulin detection and secretion assays

For immunohistochemistry, pancreatic sections (8 μm) were deparaffinized and antigens retrieved (EDTA 10 mM pH 8, 96 °C/20 min). Sections were incubated with antibodies against insulin (ab7842, 1:100, Abcam, UK), and Alexa Fluor488-conjugated

secondary antibodies (A11073, 1:1000, Thermofisher, USA) and nuclei stained with DAPI. Fluorescence was visualized with a fluorescence microscope (AxioScope A1, Zeiss, Germany) equipped with a digital camera (Canon EOS Rebel T3, Japan). The mean fluorescence intensity was obtained using ImageJ (NIH Image, http://www.scioncorp.com, Scion Corporation, USA). The area of 6–8 sections per sample was measured [33]. Fluorescence was normalized to the islet size and tissue area and to background fluorescence.

Min6 cells (p38–41) were incubated with cholesterol and/or QUE for 6 h, in serum-free and glucose-free DMEM. Cells were placed in serum free DMEM with high glucose (25 mM) for 1 h and insulin levels in the medium were measured using a Rat Ultrasensitive Insulin ELISA kit. Basal insulin secretion in the absence of glucose was also measured.

2.5. Cell viability quantification

Cell viability was assessed with the MTS assay (CellTiter 96® AQueous assay,) and by lactate dehydrogenase (LDH) release (CytoTox-ONE™ assay, both from Promega, WI, USA) in 96-well plates [4].

2.6. Apoptosis measurements

Apoptosis was assayed by measuring the activities of caspase-3 and -9, cytochrome c release and DNA fragmentation in cells plated in 6-well plates. The catalytic activity of caspase-3 and caspase-9 was colorimetrically determined using a kit from Millipore (MA, USA). To confirm the specific induction of the activities of the caspases by cholesterol, samples were also incubated for 10 min with Ac-DEVD-CHO or Ac-LEHD-CHO, specific caspase-3 and caspase-9 inhibitors, respectively [4,15]. Cytochrome c was measured using an ELISA assay (Life Technologies, CA, USA) [15]. DNA fragmentation was assessed by terminal deoxynucleotide transferase (TdT)-mediated dUTP nick end-labeling (TUNEL) coupled to FITC fluorescence (*in situ* Cell Death Detection Kit, Roche, Penzberg, Germany) [4]. Cells treated with DNase I served as positive controls. The mean fluorescence intensity was obtained with ImageJ. Images were captured in fields with 50% confluence based on DAPI staining (0.15 μg/ml).

2.7. Mitochondrial function studies

Mitochondrial function was assayed in cells in 24-well plates. MMP was evaluated using Rhod 123 [4]. ATP levels were measured using the CellTiter-Glo kit [4,34]. Oxygen consumption rates (OCR) were evaluated with an oxygraph using a Clark-type polarographic electrode (Warner Instruments, Hamden, CT, USA) and an XF^{e}96 Extracellular Flux Analyzer (Seahorse Bioscience, MA, USA). After treatment, cells were placed in a microchamber with media containing 200 mM mannitol, 5 mM KH_2PO_4, 2.5 mM $MgCl_2$, 20 mM HEPES and 0.5 mM EGTA pH 7.4 and basal OCR was registered in the oxygraph. After treatment, cells plated in XF^{e}96 were incubated for 1 h at 37 °C in XF Assay Modified Medium (25 mM glucose, 2 mM L-glutamine, 2 mM pyruvate, pH 7.4). Rotenone plus *anti*mycin A (1 μM each) were added to block complex I and III to determine the non-mitochondrial OCR, which was subtracted before calculations of mitochondrial parameters [35]. Basal OCR (state 3), state 4o (induced with 2 μM oligomycin, an ATP synthase inhibitor) and maximal OCR (State 3u, stimulated with 1.5 μM FCCP, a mitochondrial inner membrane uncoupler that allows for maximum electron flux through the electron transport chain) were sequentially measured. Maximal OCR, reserve capacity (State 3u- State3) and ATP-linked OCR (State 3-state 4o), the difference between the basal OCR and the oligomycin-insensitive OCR yields the amount of oxygen consumption that is ATP-linked) were calculated as previously described [35]. Reserve capacity is defined as the amount of oxygen consumption that is available for cells to use in times of increased ATP demand or during other stress [35,36].

2.8. Cellular redox status and antioxidant defences evaluation

Cells in 24-well plates were pre-incubated for 30 min with 50 μM dichlorodihydrofluorescein diacetate (DCFD), 10 μM dihydroethidium (DHE) or 5 μM MitoSox™ for the detection of intracellular reactive oxygen species (ROS), superoxide radicals and mitochondrial superoxide radical production, respectively, and then incubated with cholesterol and/or QUE. DHE and MitoSox™ Red assays were also conducted in the presence of SOD (100 U/ml) as a negative control for superoxide radical-dependent oxidation. Oxidative stress in pancreas and Min6 cells was evaluated by measuring lipid peroxidation using a TBARS assay kit (Cayman Chemicals, MI, USA).

SOD and GSH peroxidase activities were determined using colorimetric kit assays (Cayman). Cytosolic and mitochondria extracts were prepared as previously described [37].

2.9. qPCR measurements

The mRNA levels of *Sirt1*, *PGC-1α*, *PPAR* γ and *LXRα* were evaluated by qPCR [38]. The relative fold expression of each gene is relative to the cycle thresholds of two housekeeping genes, *Actb and GADPH* for pancreas, and *Hmbs* and *Tbp* for Min6 cells. Primer sequences are provided in supplementary Table 1.

2.10. Inflammatory status evaluation

Cytokines were measured in rat plasma and in Min6 cell homogenates using the RECYTMAG-65K and MCYTOMAG-70K Cytokine/Chemokine Magnetic Bead Panel (EMD Millipore Corporation, MI, USA). To evaluate NFκB translocation, nuclei were extracted from Min6 cells and pancreatic tissue and an NFκB (p65) Transcription Factor Assay Kit was used to assess NFκB p50 and p65 DNA binding activities (Cayman).

2.11. Statistical analysis

Data were analyzed by one-way or two-way ANOVA, followed by Bonferroni´s Multiple Comparison Test using GraphPad Prism 6 (La Jolla, CA, USA). Unless indicated otherwise, the experiments were performed three times (three independent culture preparations for the *in vitro* studies) and in triplicate or quadruplicate. Values are expressed as mean ± SEM.

3. Results

3.1. Quercetin prevented cholesterol-induced alterations in glycemic control

Four weeks of high-cholesterol (HC) feeding in rats resulted in a 74% increase in total plasma cholesterol levels and a 161% increase in the amount of cholesterol in pancreatic tissue (two-way ANOVA, post-tests $p < 0.001$, Fig. 1A and supplementary Fig. 1, all $n=8$ rats/group). HC increased the LDL and VLDL plasma levels by 114% and 100%, respectively and reduced the HDL plasma levels by 63% (all two-way ANOVA, post-test $p < 0.001$, Fig. 1B-D, all $n=8$ rats/group). The HC diet increased plasma glucose levels in fasted rats by 36% and the AUC after the IPGTT by 47% relative to the control diet (all two-way ANOVAs, post-tests $p < 0.001$, Fig. 1E and $p < 0.01$ Fig. 1G, all $n=8$ rats/group). In fasted rats, the HC diet

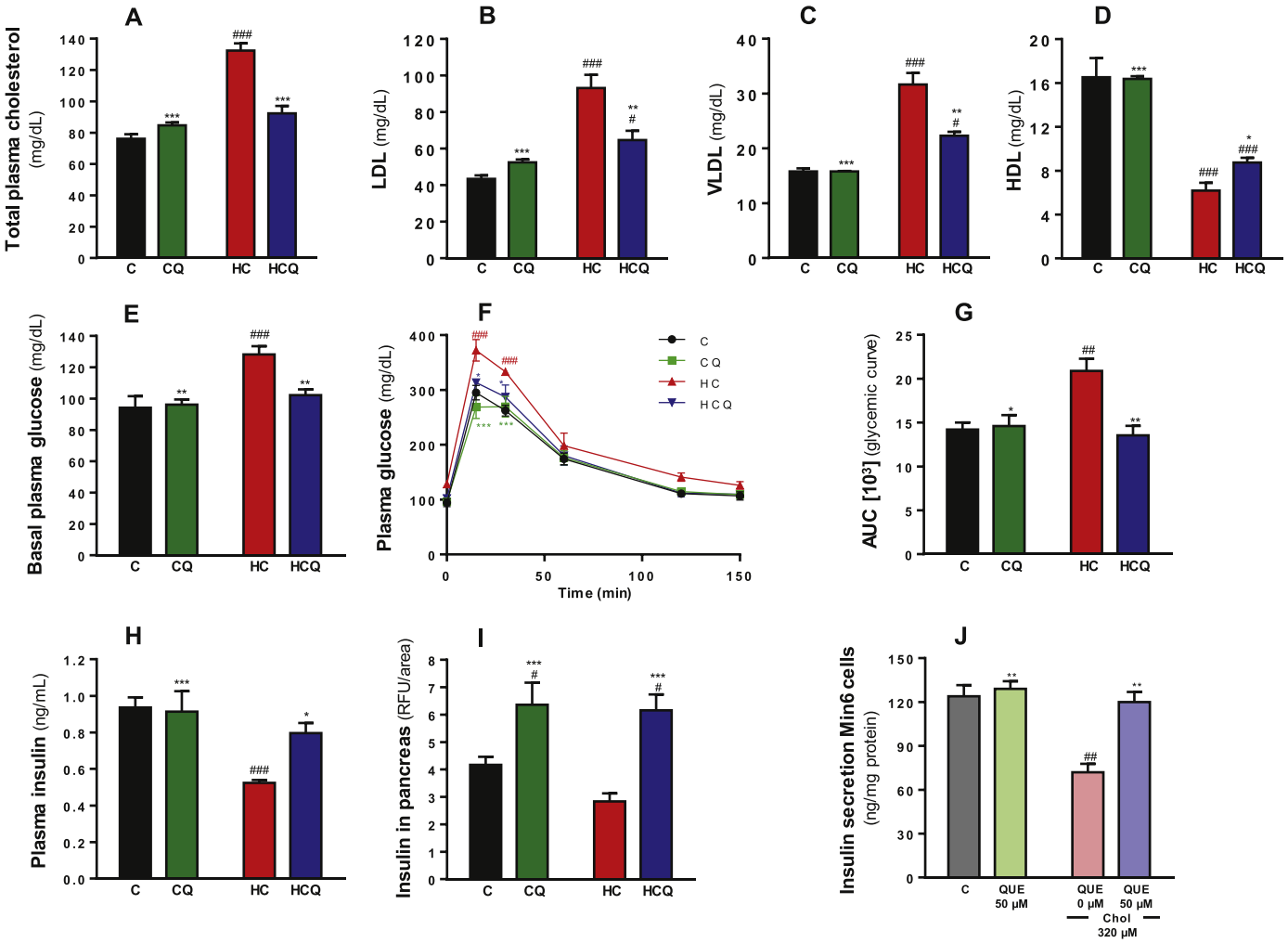

Fig. 1. Quercetin protects against the alteration on glucose and insulin levels in plasma, and pancreatic islet insulin levels induced by a high cholesterol diet and against impairments of glucose-stimulated insulin secretion in Min6 cells exposed to cholesterol. Rats were fed for 4 weeks with control diet (C), control diet containing 0.5% quercetin (CQ), high cholesterol diet (HC) or high cholesterol diet containing 0.5% quercetin (HCQ). A) Plasma glucose levels were measured after 12 h fasting. B) Results of an intraperitoneal glucose tolerance test are shown for rats fed C diet (●), CQ (■), HC (▲) and HCQ (▼), in which plasma glucose levels were recorded at 0, 15, 30, 60, 120 and 150 min after glucose ip. injection and C) the area under the curve (AUC) was calculated. D) Insulin levels in plasma and E) in pancreatic islets were measured after 12 h fasting. The fluorescence of the insulin was normalized to the Islet and tissue areas. Values are expressed as mean ± SEM. N=6–8 rats/group. F) Insulin levels in the media of Min6 cells were determined in response to glucose (25 mM, for 1 h) after 6 h incubation with 320 μM cholesterol (Chol) and/or 50 μM QUE. Values are expressed as mean ± SEM, from three independent culture preparations, each treatment performed in quadruplicate. All two-way ANOVAs, symbols indicate Bonferroni post-test significances #relative to control diet and *to HC diet or #relative to control and *to cholesterol-treated Min6 cells.

decreased insulin levels in plasma by 45% (two-way ANOVA, post-test $p < 0.001$, n=8 rats/group, Fig. 1H) and total insulin in islets of Langerhans by 25% compared to the control diet (*t* test $p=0.006$, n=8 rats/group, Fig. 1I and supplementary Fig. 2). Quercetin totally prevented the HC-induced alteration in the plasma levels of cholesterol, glucose and insulin as well as the pancreatic cholesterol content (post-test relative to HC diet $p < 0.001$, Fig. 1A; $p < 0.01$, Fig. 1B and 1D; $p < 0.05$, Fig. 1E; $p < 0.001$, Fig. 1F; and $p < 0.01$, supplementary Fig. 1). However, QUE only prevented the increase in LDL by 57% and VLDL by 59% (all two-way ANOVA, post-test $p < 0.05$ respect to Control diet and $p < 0.01$ respect to HC diet, Fig. 1B and C) and prevented the decrease in HDL by 25% (two-way ANOVA, post-test $p < 0.001$ respect to Control diet and $p < 0.05$ respect to HC diet, Fig. 1D). Quercetin had no effect when supplemented to rats in the control diet, but it increased the insulin amounts in islets by 35% (post-test relative to C diet $p < 0.05$, Fig. 1F and supplementary Fig. 2).

Ezetimibe completely inhibited the effects of HC feeding on the plasma levels of total cholesterol, basal glucose and insulin in fasted rats as well as it prevented the increase in the amount of cholesterol in pancreatic tissue (Supplementary Fig. 3A-D). Ezetimibe also prevented the alteration in lipid profile and the slightly decrease in total insulin in islets induced by the HC diet (data not shown). The data for fasting glucose and insulin levels in the five tested groups were reproduced in a second batch of 40 animals. After 2 weeks administration of HC diet the fasting glucose levels was not significant different to those with the control diet (data not shown).

Exposure of Min6 cells to cholesterol caused a 42% decrease in GSIS (two-way ANOVA, post-test $p < 0.01$, Fig. 1J), which was completely prevented by QUE (post-test relative to cholesterol $p < 0.01$). Basal secretion of insulin (without glucose) was 5 ± 0.09 ng/mg protein and was increased 10-fold in response to 25 mM glucose. Altogether, our data suggest that QUE improves glycemic control preventing the cholesterol-induced GSIS impairments in β-cells.

3.2. Quercetin protected against cholesterol-induced loss of cell viability

Cholesterol decreased the capacity of Min6 cells to reduce MTS cells by 50% and increased the leakage of LDH into the cell culture

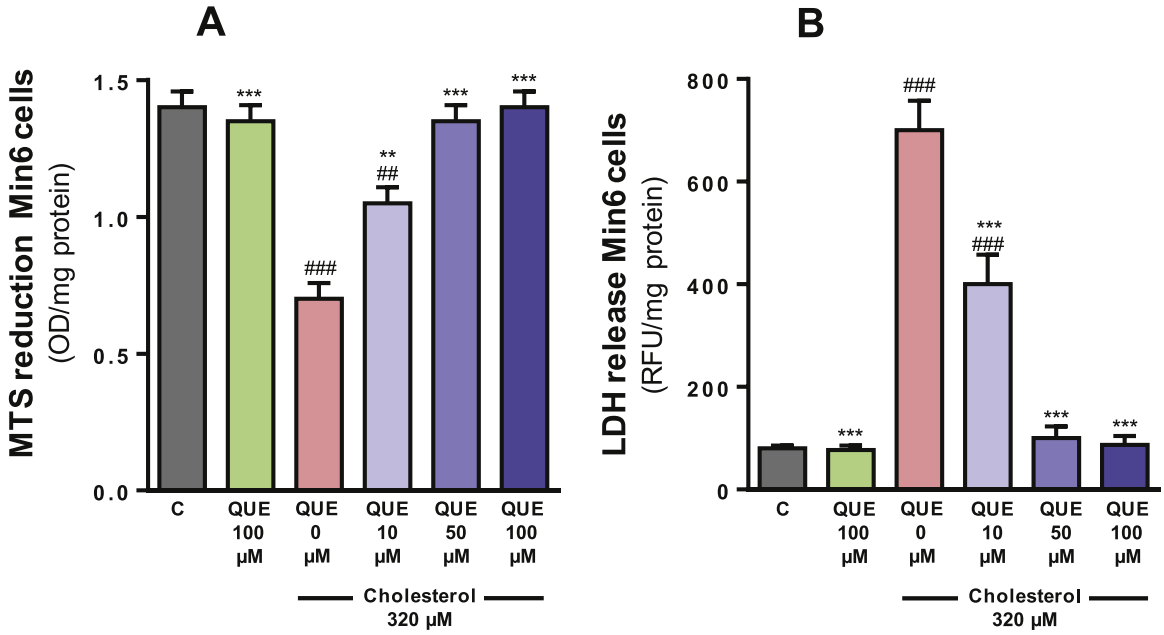

Fig. 2. Quercetin protects against cholesterol-induced decrease in Min6 cell viability. Cell viability was assessed through (A) changes in cellular MTS reduction and (B) release of LDH into the media. Cells were incubated for 6 h with 320 μM cholesterol and/or 10–100 μM QUE. MTS reduction was measured in attached cells and LDH in the supernatant. Values are expressed as mean ± SEM, from three independent culture preparations, each treatment performed in quadruplicate. All one-way ANOVA (p values specified in results), symbols indicate Bonferroni post-test significances #in comparison to control and * to cholesterol-treated Min6 cells.

medium by 8.7-fold when compared to the control cells (both one-way ANOVAs $p < 0.001$, post-tests $p < 0.001$, Fig. 2A and B). Quercetin attenuated the effects of cholesterol in a concentration dependent manner from 10 to 50 μM. The cholesterol-induced cytotoxicity was partially prevented by 10 μM QUE (post-test relative to cholesterol and control $p < 0.01$, Fig. 2A and $p < 0.001$, Fig. 2B) and completely prevented by 50 μM QUE ($p < 0.001$, Fig. 2A and B).

3.3. Quercetin inhibited cholesterol-induced apoptosis

Cholesterol increased the activities of caspase-3 by 140% and caspase-9 by 137% as well as the cytochrome c release by 82% when compared to the control Min6 cells (all one-way ANOVAs $p < 0.001$, post-tests $p < 0.001$, Fig. 3A-C). DNA fragmentation was enhanced by 120% relative to the control cells (one-way ANOVA $p < 0.001$, post-test $p < 0.001$, Fig. 3D and E). Quercetin prevented these increases in caspase activities and cytochrome c release in a concentration-dependent manner. Complete attenuation of cholesterol-induced apoptosis was achieved with 50 μM QUE (post-test relative to cholesterol $p < 0.001$, all parameters, Fig. 3A-E). In the presence of DEVD-CHO or LEHD-CHO, inhibitors or caspases-3 and 9 respectively, cholesterol did not cause caspase activation (Fig. 3A and B).

3.4. Quercetin prevented cholesterol-induced mitochondrial bioenergetic dysfunction

HC diet decreased the ATP levels in pancreatic tissue by 43% compared to the control diet (two-way ANOVA, post-test $p < 0.05$, $n = 8$ rats/group, Fig. 4A), which was completely prevented with QUE supplementation (post-test relative to HC diet $p < 0.05$, Fig. 4A). Adding QUE to the control diet caused no changes in ATP levels (Fig. 4A). Ezetimibe also fully inhibited the HC-induced drop in pancreatic ATP levels (data not shown). Cholesterol decreased the ATP levels in Min6 cells by 32% and the MMP by 48% when compared to the control cells (one-way ANOVAs $p < 0.001$, post-tests $p < 0.01$, Fig. 4B and $p < 0.001$, Fig. 4C). 10 μM QUE completely protected against the cholesterol-induced decrease in ATP levels (post-test relative to cholesterol $p < 0.05$, Fig. 4B) and partially against the decrease of MMP in Min6 cells (post-test relative to cholesterol and to control $p < 0.05$, Fig. 4C); while complete protection was achieved at 50 μM QUE (post-test relative to cholesterol $p < 0.001$, Fig. 4C). An example of a coupling assay measuring OCR using the XF^{e}96 Analyzer is shown in Fig. 4D. Cholesterol decreased basal OCR by 40%, maximal OCR by 38%, ATP-linked OCR by 63% and reserve capacity by 62% in Min6 cells compared to the control (all two-way ANOVAs, post-tests $p < 0.01$, Fig. 4E-H). Ten μM QUE prevented the mitochondrial OCR impairments induced by cholesterol, while by itself also improved the basal and maximal OCRs, ATP-linked OCR and the reserve capacity by 41%, 26%, 100% and 83%, respectively (post-test relative to cholesterol and to control $p < 0.01$, Fig. 4E-H). The basal OCRs obtained from the XF^{e}96 Analyzer (Fig. 4E) were reproduced by polarography (data not shown).

3.5. Quercetin reduced cholesterol-induced oxidative stress

Cholesterol increased the levels of intracellular ROS by 120%, cytosolic superoxide radicals by 122%, mitochondrial superoxide radicals by 168%, lipid peroxidation by 88% in Min6 cells when compared to control (all one-way ANOVAs $p < 0.001$; post-tests $p < 0.001$, Fig. 5A-D). HC diet also increased lipid peroxidation by 122% in pancreas (two-way ANOVA, post-test $p < 0.001$, Fig. 1E, all $n = 8$ rats/group). While QUE had no effect on these measurements in the absence of cholesterol, it prevented the oxidative stress and lipid peroxidation induced by cholesterol in a concentration-dependent manner in Min6 cells. Ten μM was sufficient to completely prevented these oxidative stress indicators (post-test relative to cholesterol $p < 0.001$, all parameters, Fig. 5A-C; $p < 0.05$, Fig. 5D). Quercetin also prevented the lipid peroxidation induced by HC diet in pancreas (post-test relative to cholesterol $p < 0.001$, Fig. 5E). In the presence of SOD, cholesterol did not oxidise DHE and MitoSox probes (Fig. 5B and C), indicating that in Min6 cells cholesterol promotes the production of superoxide radicals which selectively oxidise the used probes.

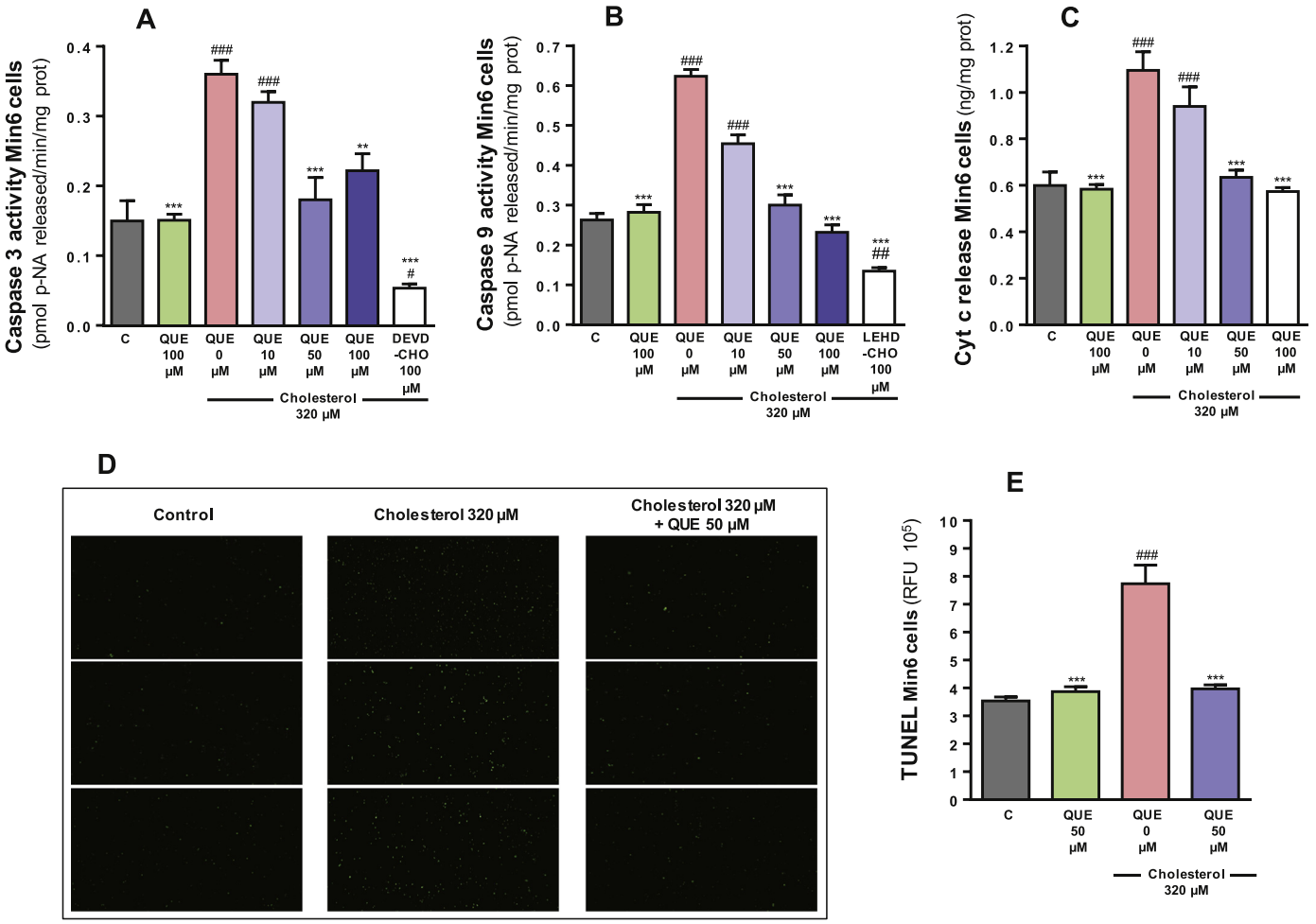

Fig. 3. Quercetin protects against cholesterol-induced apoptosis of Min6 cells. The activities of (A) caspase-3 and (B) caspase-9 were measured after 6 h incubation with 320 μM cholesterol and/or 10–100 μM QUE. Cholesterol was also incubated with specific caspase inhibitors, DEVD-CHO and LEHD-CHO, respectively. (C) Cytochrome c release was quantified in media from cells treated for 6 h with 320 μM cholesterol and/or 10–100 μM QUE. (D) TUNEL staining after 6 h incubation with 320 μM cholesterol and/or 50 μM QUE. (E) Quantification of DNA fragmentation. Values are expressed as mean ± SEM, from three independent culture preparations, each treatment performed in triplicate. All one-way ANOVA (p values specified in results), symbols indicate Bonferroni post-test significances #relative to control and *to cholesterol-treated Min6 cells.

3.6. Quercetin protected cholesterol-induced decrease in antioxidant defences

In the pancreas, HC diet decreased cytosolic activities of SOD by 70% and GSH peroxidase by 69%, when compared to the control diet (all two-way ANOVAs, post-tests $p < 0.01$, Fig. 6A and $p < 0.05$, Fig. 6B, all $n = 8$ rats/group). HC diet also decreased the mitochondrial activities of SOD and GSH peroxidase by 65% and 62% respectively (two-way ANOVA, post-test $p < 0.01$, $n = 8$ rats/group, Fig. 6C and D). Quercetin completely prevented the HC-induced decrease in antioxidant enzyme activities (post-tests relative to HC diet $p < 0.001$, Fig. 6A; $p < 0.01$, Fig. 6B and D; $p < 0.05$, Fig. 6C). Similar to QUE, Ezetimibe also completely prevented the effects of HC on the antioxidant enzymatic activities in pancreatic tissue (data not shown).

In Min6 cells, cholesterol decreased the total activity of SOD by 57% and GSH peroxidase by 48% when compared to control Min6 cells (all one-way ANOVAs $p < 0.001$, post-tests $p < 0.05$, Fig. 6E, and $p < 0.01$ Fig. 6F). Quercetin (10 μM) completely reversed the decrease in the antioxidant enzyme activities induced by cholesterol (post-tests relative to cholesterol $p < 0.01$, Fig. 6E and $p < 0.05$, Fig. 6F).

3.7. Quercetin decreased cholesterol-induced inflammation

When compared to control diet, the HC diet caused a 140% increase in NFκB translocation to the nucleus in pancreas (two-way ANOVA, post-test $p < 0.01$, $n = 8$ rats/group, Fig. 7A) and an increase in the expression of cytokines downstream of NFκB activation (Table 1). The HC diet increased the plasma levels of IL-1β by 151% TNF-α by 72%, IFN-γ by 49% and granulocyte-macrophage colony-stimulating factor (GM-CSF) by 946% (all two-way ANOVAs, post-tests $p < 0.01$, $n = 6–8$ rats/group, Table 1). Quercetin prevented the HC-induced increase in pancreatic NFκB translocation (post-test relative to HC diet $p < 0.05$, Fig. 7A) and in pro-inflammatory cytokine levels in plasma (post-test relative to HC diet $p < 0.001$, IL-1β; $p < 0.05$, TNF-α; $p < 0.001$, IFN-γ; $p < 0.01$, GM-CSF; Table 1). Quercetin had no effect when added to the control diet (Fig. 7A and Table 1). Ezetimibe totally prevented the inflammatory effect of HC in NFκB activation and cytokine levels (data not shown).

In Min6 cells cholesterol increased the NFκB translocation to the nucleus by 39% (one-way ANOVA $p = 0.0002$, post-test $p < 0.05$, Fig. 7B) and the levels of IL-1β by 14%, TNF-α by 15%, IFN-γ by 19% and GM-CSF by 42% when compared to the control Min6 cells (two-way ANOVAs, post-tests $p < 0.05$, Table 1). At 10 μM, QUE was able to completely inhibit the increase in NFκB translocation (post-test relative to cholesterol $p < 0.05$, Fig. 7B). At 50 μM,

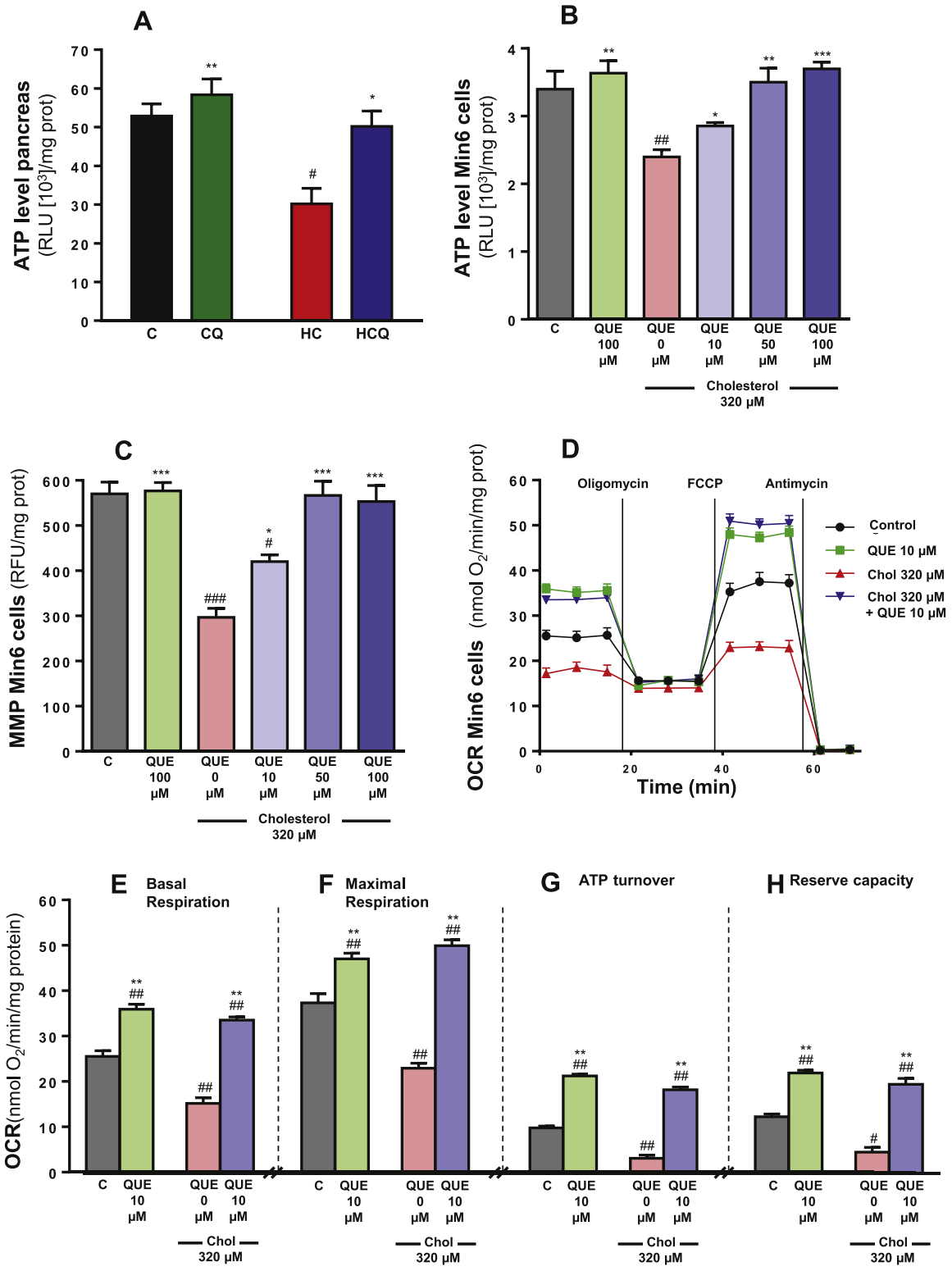

Fig. 4. Quercetin protects against the decrease in ATP levels in pancreas of rats fed high cholesterol diet and mitochondrial dysfunction in Min6 cells exposed to cholesterol. Rats were fed for 4 weeks with control diet (C), control diet containing 0.5% quercetin diet (CQ), high cholesterol diet (HC) and high cholesterol diet containing 0.5% quercetin (HCQ).A) ATP levels were measured in pancreas after 12 h fasting. N=6–8 rats/group. Two-way ANOVA, symbols indicate Bonferroni post-test significances #relative to control diet and *to HC diet. Min6 cells were incubated with 320 µM cholesterol and/or 10, 50 or 100 µM QUE. After 6 h B) the ATP, C) MMP levels, and D-H) mitochondrial respiration parameters were evaluated and expressed as nmol/min/mg prot. (D) Mitochondrial functions were measured in the form of OCR and expressed as nmol of oxygen consumed/min/mg protein using the Seahorse XF^{e}96 analyzer in control cells (●) or 6 h-treated cells with: 10 µM QUE (■), 320 µM cholesterol (▲) or 320 µM cholesterol (Chol)+10 µM QUE (▼). (E) Basal OCR and (F) maximal OCR stimulated with FCCP (State 3 u) are shown. (G) ATP-linked OCR was calculated from basal OCR minus the oligomycin-insensitive OCR. (H) Reserve capacity was calculated as maximal minus basal OCR. Values are expressed as mean ± SEM, from three independent culture preparations, each treatment performed in quadruplicate. One-way ANOVAs (B and C, p values specified in results) and two-way ANOVAs (E-H), symbols indicate Bonferroni post-test significances # in comparison to control and *to cholesterol-treated Min6 cells. Chol, cholesterol; OCR, oxygen consumption rate; RLU, relative luminescence unit.

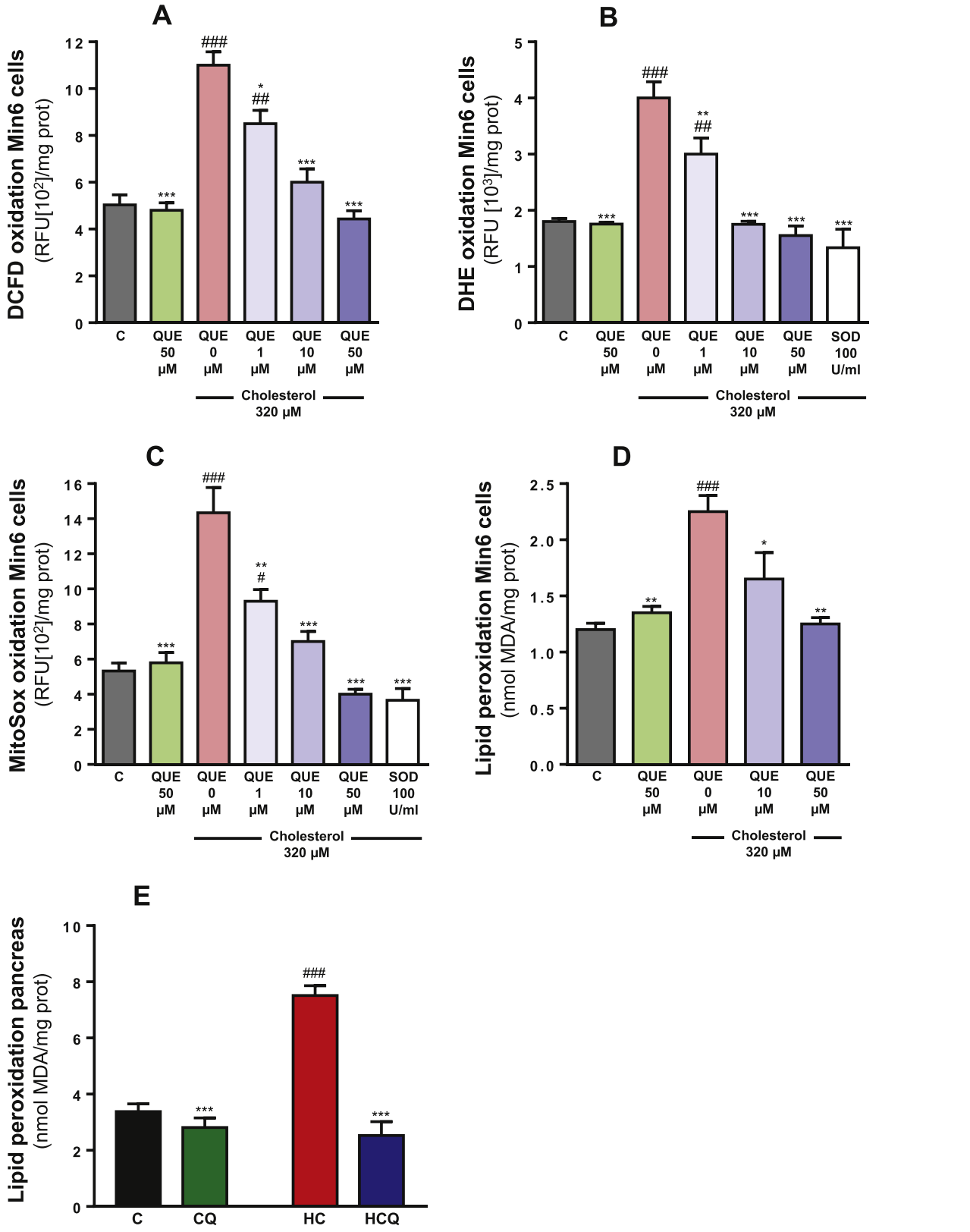

Fig. 5. Quercetin protects against cholesterol-induced oxidative stress in Min6 cells. After treatment of Min6 cells for 6 h with 320 μM cholesterol and/or 1, 10, 50 or 100 μM QUE, cellular oxidative status was determined through (A) DCFD oxidation and (B) DHE oxidation. (C) Mitochondrial and oxidative status was determined using MitoSox™ Red oxidation. Oxidative stress was determined by measuring lipid oxidation by TBARS (D) in Min6 cells and (E) in pancreas. Values are expressed as mean ± SEM, from three independent culture preparations, each treatment performed in quadruplicate. All one-way ANOVA (p values specified in results), symbols indicate Bonferroni post-test significances #relative to control and *to cholesterol-treated Min6 cells. MDA, malondialdehyde.

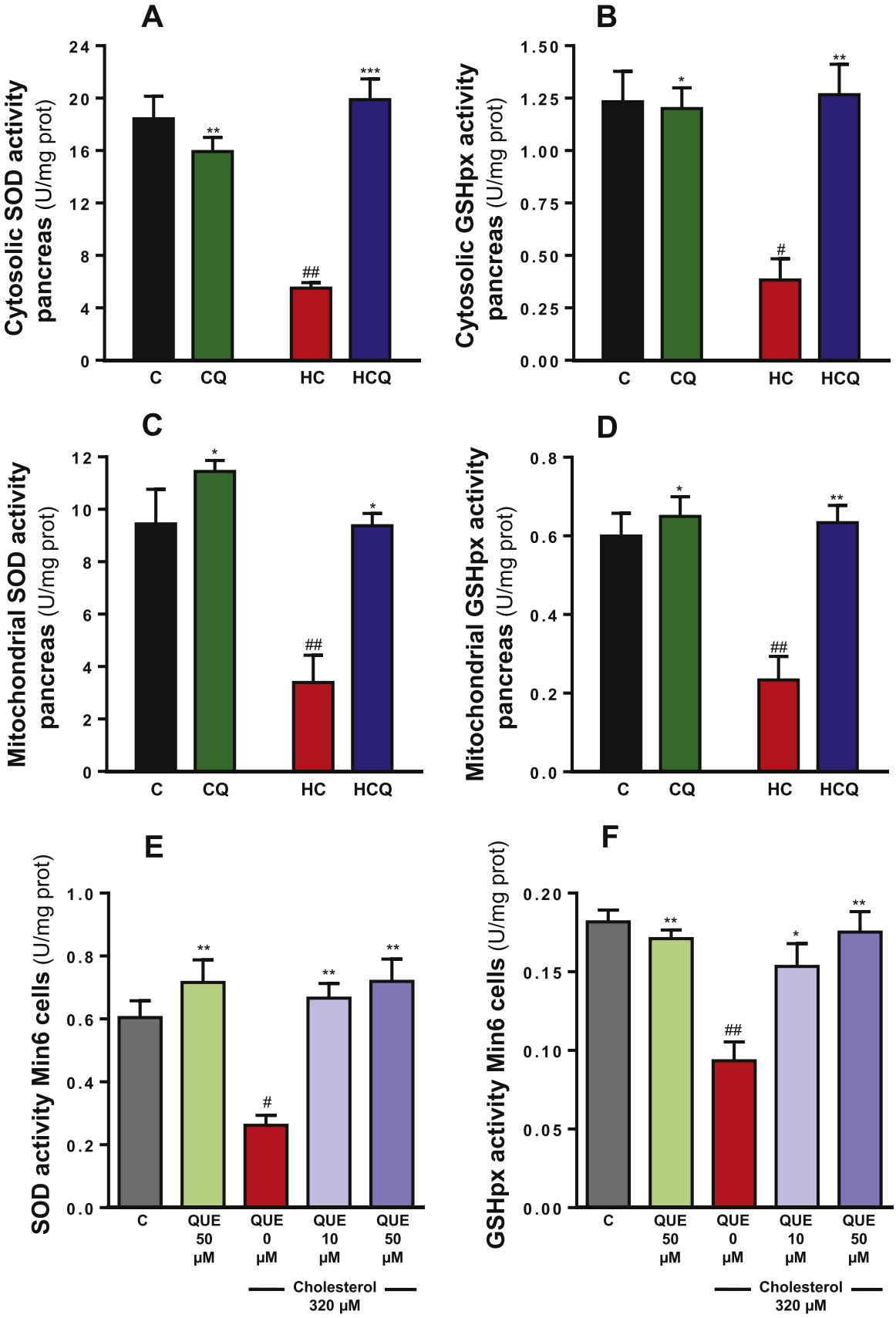

Fig. 6. Quercetin protects against the decrease in enzymatic antioxidant defences in the pancreas from rats fed high cholesterol diet and in Min6 cells exposed to cholesterol. In pancreas from rats fed for 4 weeks with control diet (C), control diet containing 0.5% quercetin diet (CQ), high cholesterol diet (HC) and high cholesterol diet containing 0.5% quercetin (HCQ) the cytosolic activities of (A) SOD and (B) glutathione peroxidase, and the mitochondrial activities of (C) SOD and (D) glutathione peroxidase were assessed after 12 h fasting. N= 6–8 rats/group. Two-way ANOVAs (A-D), symbols indicate Bonferroni post-test significances #relative to control diet and *to HC diet. In cells incubated for 6 h with320 µM cholesterol and/or 10 or 50 QUE, the (E) SOD and (F) glutathione peroxidase activities were measured in the whole cell homogenate. Values are expressed as mean ± SEM, from three independent culture preparations, each treatment performed in quadruplicate. One-way ANOVAs (p values specified in results), symbols indicate Bonferroni post-test significances #with respect to control and *to cholesterol-treated Min6 cells.

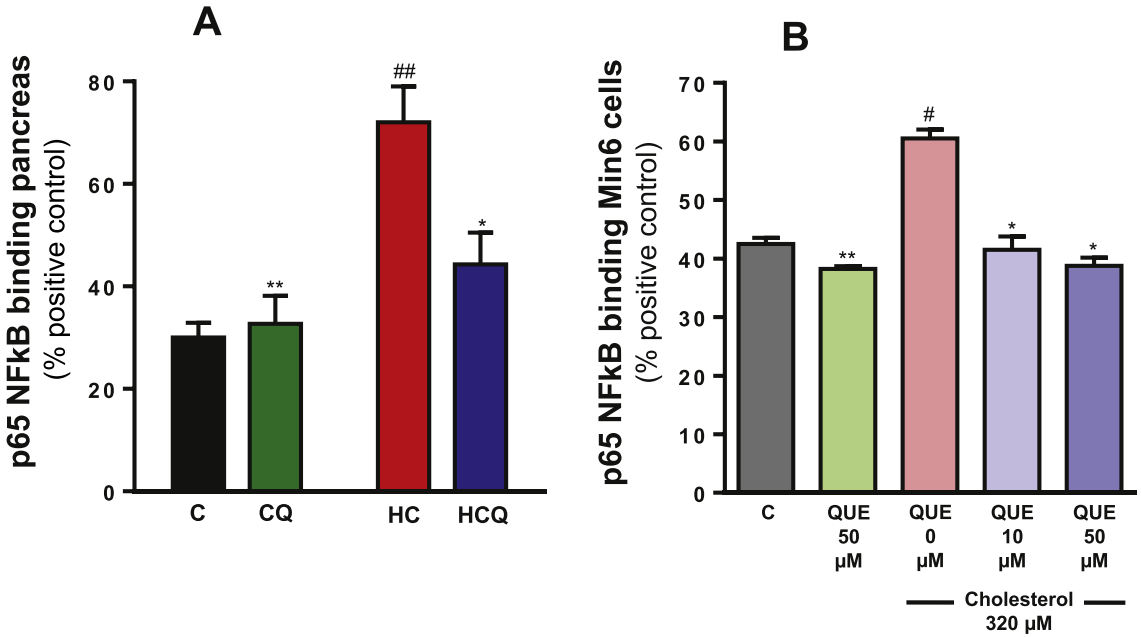

Fig. 7. Quercetin protects against the increase in NFκB translocation to the nucleus in the pancreas from rats fed high cholesterol diet and in Min6 cells exposed to cholesterol. Nuclear extracts from A) pancreas of rats fed for 4 weeks with control diet (C), control diet containing 0.5% quercetin (CQ), high cholesterol diet (HC) and high cholesterol diet containing 0.5% quercetin (HCQ) and B) nuclear extracts from cells incubated for 6 h with 320 μM cholesterol and/or 50 μM QUE and NFκB (p65) were quantified. Values are expressed as percentage relative to positive control (HeLa cell lysate containing TNFα-activated NFκB (p65), 100%). Values are expressed as mean ± SEM. N = 6–8 rats/group. In the vitro study three independent culture preparations were assessed, in which each treatment was performed in quadruplicate. All two-way ANOVAs, symbols indicate Bonferroni post-test significances $^{\#}$compared to control diet and *to HC diet; or $^{\#}$relative to control and *to cholesterol-treated Min6 cells.

QUE attenuated the increase in the pro-inflammatory cytokine levels (post-test relative to cholesterol $p < 0.01$, IL-1β and IFN- γ; $p < 0.05$, TNF-α; $p < 0.001$g-CSF; Table 1). In the absence of cholesterol, QUE had no effect in most of these pro-inflammatory parameters (Fig. 7B and Table 1). Quercetin, with or without cholesterol, caused a decrease in GM-CSF levels by around 20% (post-test relative to control $p < 0.001$).

Cholesterol and QUE did not alter the plasma levels of these pro-inflammatory cytokines: IL-1α, IL-6, macrophage inflammatory protein 1 alpha (MIP-1α) and keratinocyte-derived chemokine (KC) in Min6 cells (data not shown). Quercetin, with and without cholesterol, decreased the plasma levels of IL-12 by 16%, monocyte chemoattractant protein-1 (MCP-1) by 14%, IL-5 by 30%, IL-7 by 16% and MIP-2 by 44% approximately in Min6 cells (data not shown).

3.8. Quercetin modulated cholesterol-induced alteration in gene expression

Compared to control diet, the HC diet decreased the expression of *Sirt1* by 87% (two-way ANOVA, post-test $p < 0.001$, Table 2) and increased the expression of *PGC-1α* by 98% (two-way ANOVA, post-test $p < 0.05$, Table 2), *PPAR* γ by 68% (two-way ANOVA, post-test $p < 0.01$, Table 2) and *LXRα* by 89% (two-way ANOVA, post-test $p < 0.01$, Table 2). The QUE supplemented control diet (CQ) increased the expression of *Sirt1* and *PGC-1α* by 54% and 154% relative to control diet, respectively (post-test relative to control diet $p < 0.01$, *Sirt1* and $p < 0.05$, *PGC-1α*, Table 2). When added to the HC diet, QUE (HCQ) increased the expression of *Sirt1* and *PGC-1α* by 51% and 230% respectively when compared to the control diet (post-test relative to control diet $p < 0.05$, *Sirt1* and $p < 0.001$, *PGC-1α*, Table 2) and by 288% and 67% when compared to HC diet

Table 1
Quercetin prevents the increase of cytokines induced by cholesterol: *in vivo* and *in vitro* studies.

Plasma				
pg cytokines/ml plasma	**C**	**CQ**	**HC**	**HCQ**
IL-1β	15.54 ± 5.52	4.91 ± 1.54***	38.93 ± 7.11##	2.63 ± 1.33***
TNF-α	1.63 ± 0.28	1.79 ± 0.29*	2.81 ± 0.24##	1.94 ± 0.28*
IFN-γ	42.91 ± 2.36	35.13 ± 1.01*	63.81 ± 8.65#	25.06 ± 6.34***
GM-CSF	3.39 ± 0.76	3.47 ± 0.76*	35.49 ± 12.45##	2.88 ± 0.10**
Min6 cells				
pg cytokines/mg protein	**Control**	**Quercetin 50 μM**	**Cholesterol 320 μM**	**Quercetin 50 μM + Cholesterol 320 μM**
IL-1β	70.30 ± 0.97	73.97 ± 1.39*	79.86 ± 0.63###	73.05 ± 1.33**
TNF-α	13.06 ± 0.34	13.02 ± 0.46*	15.04 ± 0.44##	13.44 ± 0.18*
IFN-γ	29.94 ± 0.69	30.64 ± 0.99*	35.54 ± 1.54#	29.12 ± 1.67**
GM-CSF	119.1 ± 2.01	92.36 ± 5.12***,##	168.6 ± 2.30###	93.67 ± 6.02***,##

Pro-inflammatory markers in plasma from rats fed control diet (C), control diet containing 0.5% quercetin (CQ), high cholesterol diet (HC) and high cholesterol diet containing 0.5% quercetin (HCQ). Values are expressed as mean ± SEM. N = 6–8 rats/group.
Pro-inflammatory markers in Min6 cells treated for 20 h with 320 μM cholesterol and/or 50 μM QUE. Values are expressed as mean ± SEM, from three independent culture preparations, each treatment performed in quadruplicate. All two-way ANOVA, symbols indicate Bonferroni post-test significances $^{\#}$in comparison to control and *to (high)-cholesterol.$^{*}p < 0.05$, $^{**}p < 0.01$, $^{***}p < 0.001$; $^{\#}p < 0.05$, $^{\#\#}p < 0.01$, $^{\#\#\#}p < 0.001$.

Table 2
Quercetin and cholesterol modulate gene expression: *in vivo* and *in vitro* studies.

Pancreas				
Gene [relative fold expression]	**C**	**CQ**	**HC**	**HCQ**
Sirt1	1.00 ± 0.07	$1.54 \pm 0.15^{***,\#\#}$	$0.13 \pm 0.07^{\#\#\#}$	$1.51 \pm 0.12^{***,\#}$
PGC-1α	1.00 ± 0.19	$2.54 \pm 0.50^{**,\#}$	$1.98 \pm 0.11^{\#}$	$3.30 \pm 0.36^{**,\#\#\#}$
PPAR γ	1.00 ± 0.13	$0.30 \pm 0.02^{***,\#\#}$	$1.68 \pm 0.21^{\#\#}$	$1.15 \pm 0.03^{*}$
LXRα	1.00 ± 0.11	$0.30 \pm 0.07^{***,\#}$	$1.89 \pm 0.31^{\#\#}$	$0.99 \pm 0.06^{**}$
Min6 cells				
Gene [relative fold expression]	**Control**	**Quercetin 50 μM**	**Cholesterol 320 μM**	**Quercetin 50 μM + Cholesterol 320 μM**
Sirt1	1.00 ± 0.02	$1.35 \pm 0.07^{***,\#\#\#}$	$0.89 \pm 0.04^{\#}$	$1.33 \pm 0.12^{***,\#\#\#}$
PGC-1α	1.00 ± 0.09	$1.66 \pm 0.18^{\#\#\#}$	$1.46 \pm 0.20^{\#\#}$	$2.38 \pm 0.09^{***,\#\#\#}$
PPAR γ	1.00 ± 0.26	$0.88 \pm 0.07^{***}$	$1.77 \pm 0.17^{\#\#\#}$	$1.37 \pm 0.03^{*,\#}$

Gene expression in plasma from rats fed control diet (C), control diet containing 0.5% quercetin (CQ), high cholesterol diet (HC) and high cholesterol diet containing 0.5% quercetin (HCQ). Values are expressed as mean ± SEM. N=6–8 rats/group.
Gene expression in Min6 cells treated for 20 h with 320 μM cholesterol and/or 50 μM QUE. Values are expressed as mean ± SEM, from three independent culture preparations, each treatment performed in quadruplicate. All two-way ANOVA, symbols indicate Bonferroni post-test significances $^{\#}$in comparison to control and *to (high)-cholesterol.$^{*}p < 0.05$, $^{**}p < 0.01$, $^{***}p < 0.001$; $^{\#}p < 0.05$, $^{\#\#}p < 0.01$, $^{\#\#\#}p < 0.001$.

(post-test relative to HC diet $p < 0.001$, *Sirt1* and $p < 0.01$, *PGC-1α*, Table 2). Quercetin was able to block the HC-induced increase of *PPAR γ* (post-test relative to HC diet $p < 0.05$, Table 2) and *LXRα* expression (post-test relative to HC diet $p < 0.01$, Table 2). Furthermore, QUE decreased the expressions of *PPAR γ* and *LXRα* by 70% (post-test relative to control diet $p < 0.01$, *PPAR γ* and $p < 0.05$, *LXRα*, Table 2). All gene expression from the HC diet supplemented with ezetimibe was not significantly different to the control group (data not shown). Cholesterol and QUE had no effect in IL-12 plasma levels (data not shown).

Compared to control, Min6 cells treated with cholesterol had decreased *Sirt1* expression by 11% (two-way ANOVA, post-test $p < 0.05$, Table 2); while QUE increased its expression by around 35%, either in the presence or absence of cholesterol (two-way ANOVA, post-test relative to control and cholesterol $p < 0.001$, Table 2). Cholesterol increased the expression of *PGC-1α* by 46% and *PPAR γ* by 77% (two-way ANOVAs, post-tests $p < 0.01$, Table 2). Quercetin, with and without cholesterol, increased the expression of *PGC-1α* by 138% and 67% when compared to the control cells, respectively (post-test relative to control $p < 0.001$, Table 2). Quercetin almost totally counteracted the increase of *PPAR γ* expression induced by cholesterol (post-test relative to cholesterol and control $p < 0.05$, Table 2).

4. Discussion

In this study we found that QUE prevented the dysfunctions in plasma glucose control in rats fed high cholesterol diet and GSIS impairment in cultured pancreatic β-cells exposed to cholesterol. Using islets of Langerhans staining, Min6 cells and animal rat model, we demonstrated that QUE prevented cholesterol-induced apoptosis, mitochondrial dysfunction, oxidative stress and inflammation in both *in vitro* and *in vivo* models. Given that type 2 diabetes mellitus has become a major health issue worldwide, and it is well known that cholesterol plays an important role in pancreatic β-cell dysfunction by inducing the impairment of GSIS [3,5,9]. The novel effects of QUE described here increase the interest into QUE as a potential anti-diabetic agent.

4.1. New finding in this study

Although the effect of high cholesterol diet on cardiovascular diseases has been widely addressed, its effects on metabolic impairments, specifically on glycemic control have been scarcely studied [64–66]. While the antidiabetic effects of QUE have been shown in a streptozocin model of diabetes in rats [67], our study addresses for the first time the protective effect of QUE against impairments of glycemic control (fasting and in IPGTT) and insulin levels induced by HC diet in rats, including the mechanisms involved in pancreas and pancreatic β-cells. Here we demonstrated for the first time that HC diet results in impairments in insulin secretion/production in the islet of Langerhans, which ultimately leads to decreased plasma insulin levels and decreased glucose tolerance. Our study also identified for the first time that cholesterol alters mitochondrial bioenergetics, importantly reducing ATP-linked OCR and reserve capacity in Min6 cells. This is supported by the fact that QUE improved mitochondrial function and thus, protected against the cholesterol induced GSIS impairment, presented here as a novel mechanism of protection by this flavonoid in insulinoma cells. Although it has been shown that high fat diet and high fructose diet decrease *Sirt1* expression in pancreas [68], here we describe for the first time that high cholesterol also exerts the same effect in pancreas and in pancreatic β-cells. Through this mechanism, cholesterol may induce mitochondrial dysfunction, apoptosis and inflammation and thus, promote impairments in blood glucose control. These deleterious effects of cholesterol were abolished in the presence of QUE, which also increased *Sirt1* expression. Our findings of altered Sirt1 expression in pancreas and pancreatic β-cells are also novel.

4.2. Cholesterol alters glycemic control validating of our high cholesterol diet in vivo model

According to our *in vivo* results, the damaging effect on glycemic control induced by HC diet is attributed to the increased cholesterol levels in plasma and by the alteration of the lipid profile, increased LDL and VLDL levels and decreased HDL levels. The impairments in glycemic and insulin control (in plasma and islets) (Supplementary Fig. 2C-D) were totally prevented when the increase in total plasma cholesterol levels (and in consequence the amount of cholesterol in pancreas) and the alterations in lipid profile caused by the HC diet was reversed by the supplementation with ezetimibe (Supplementary Fig. 2A-D), a drug used to treat hypercholesterolemia that blocks NPC1L1-dependent cholesterol transport [29]. Quercetin prevented the increase in total plasma cholesterol induced by HC, but it only partially prevented the alterations in lipid profile levels, as it was recently reported in hypercholesterolemic Apo E−/− mice [39]. Thus, the partial effect of QUE on preventing the HC diet-induced increase in LDL levels, the particle that carries the majority of the cholesterol in the blood and supplies it to the cells, and in VLDL levels, which could be

converted to LDL, supports the idea that the protecting effect of QUE on the glycemic control is beyond its effect on controlling total cholesterol levels. This justifies further evaluation *in vitro*, in pancreatic beta cells and *in vivo*, in pancreas against the damage induced by cholesterol.

4.3. Quercetin protects against the mitochondrial dysfunction induced by cholesterol

Only 10 μM QUE was required to protect against cholesterol-induced mitochondrial dysfunction in Min6 (Fig. 4B-H). In line with the antioxidant potential of QUE, this was the same concentration of QUE that completely protected against cholesterol-induced oxidative stress. The powerful effect of this low concentration can be explained by earlier findings that demonstrate QUE accumulation in mitochondria, which is likely to confer QUE's exceptional potency for mitochondrial protection [15,16]. The effective concentration of QUE in our *in vitro* study (10–50 μM) is likely to be reached *in vivo*, since a bioavailability study in rats fed 0.5% QUE diet (this corresponds to the amount used in our study) for 10 days found 118 ± 8 μM of plasma QUE [40]. In addition, after 30 min of the administration of 50 mg/Kg of QUE to rats (in our study we used a ten time higher dose), a plasma concentration of 58 ± 10 μM was detected [41].

Our results suggest that cholesterol induces mitochondrial dysfunction by interfering with the electron transport chain (ETC) and altering the physiological efflux of protons from the mitochondrial matrix to the intermembrane space, thereby decreasing MMP (Fig. 4C) and interfering with oxygen consumption [42]. In line with this, we observed a decrease in basal (Fig. 4E) and maximal OCR (Fig. 4F), ATP-linked OCR (Fig. 4G) and reserve capacity (Fig. 4H) in Min6 cells that were treated with cholesterol. A decrease in ATP-linked OCR would indicate either low ATP demand, a lack of substrate availability, or severe damage to the ETC, which would impede the flow of electrons and result in a lower OCR [36]. Reduced MMP (Fig. 4C) and ATP levels (Fig. 4A-B) may trigger mitochondrial swelling by induction of the permeability transition pore, a key effector of the apoptosis pathway mediating cytochrome c release [43,44]. Consistent with this, we found that cholesterol promotes cytochrome c release (Fig. 3C). Importantly, cytochrome c release has been proposed as a biomarker of mitochondrial dysfunction associated to the intrinsic pathway of apoptosis [44]. Congruent with this, we found increased activities of caspase-3 and caspase-9 (Fig. 3A-B), and DNA fragmentation after cholesterol treatment (Fig. 3D-E). Although the mitochondrial dysfunctions induced by cholesterol may promote apoptosis through the intrinsic pathway, the contribution of the extrinsic pathway of apoptosis induced by cholesterol through the activation of death receptors cannot be ruled out [45]. In addition to the protection against cholesterol-induced apoptosis by the prevention of mitochondrial dysfunction and cytochrome c release, QUE may exert protective effects by increasing *Sirt1* expression. Sirtuin 1 regulates cell survival by deacetylating and inactivating p53 [46], and by deacetylating Ku70, thus controlling Bax activation [47].

An elevation in the ATP/ADP ratio induces exocytosis of insulin [48]. Therefore, the observed decrease in ATP levels may contribute to low insulin levels in the plasma of rats supplemented with the HC diet. This is expected to result in impairments found in GSIS (Fig. 1G) and glycemic control (Fig. 1B-D). Since the HC diet caused a higher peak in plasma glucose levels and a larger AUC in the IPGTT tolerance test, the detrimental effect of HC on glycemic control appears to be attributed to impairment in insulin production and release by the pancreas rather than to insulin resistance by adipocytes and skeletal muscles. However, it cannot be ruled out that cholesterol, in addition to its detrimental effect on mitochondrial bioenergetics, may also impair the secretion of insulin by altering membrane trafficking involved in insulin release due to an effect on membrane rigidity [49]. However, as QUE protected against cholesterol-induced impaired GSIS in a β-cell line, our data suggest that cholesterol does not directly alter membrane properties in our experimental conditions.

The conservation of a substantial bioenergetic reserve capacity is a prospective index of "healthy" mitochondrial populations, it is essential for resistance to oxidative stress and supplying ATP [36]. The higher reserve capacity in QUE treated cells (Fig. 4H) indicates that QUE improves the ability of substrate supply/oxidation and thus ETC to respond to increased energy demand, as well as providing more resistance to oxidative stress. The latter is highly relevant in insulinoma, specifically under hyperglycemic condition, as β-cells constantly have an increased energy demand when insulin is released. As QUE accumulates in mitochondria [15,16], and protects against the inhibition of complex I activity [15], it is possible that QUE may also exert a beneficial effect directly within the mitochondria. Unlike synthetic antioxidant conjugated with triphenylphosphonium (TPP^+), such as MitoQ, MitoTempol, QUE targets mitochondria without inhibiting oxidative phosphorylation [50]. The improvement of ATP-linked OCR and the reserve capacity found here are important mechanisms for the protection by QUE against the impairments in insulin regulation in plasma and in pancreas and thus against the dysfunction of GSIS and glycemic control induced by cholesterol.

Quercetin may also protect against cholesterol-induced mitochondrial dysfunction by increasing *Sirt1* expression further rather than preventing its decrease by cholesterol (Table 2). Sirtuin 1-mediates the regulation of PGC-1α activity by deacetylation [51]. PGC-1α is a key regulator of mitochondrial biogenesis, and it has been reported to induce several genes involved in the TCA cycle, antioxidant defense, ETC, as well as mitochondrial transcription factor A (Tfam), an important factor for mitochondrial DNA (mtDNA) transcription, translation, and repair [52]. Quercetin promotes an increase in *PGC-1α* expression (Table 2), but unlike that of cholesterol, it may be highly activated by the increased expression of *Sirt1* as evidenced by improved mitochondrial function observed in the presence of QUE.

In contrast, the increase in *PGC-1α* expression induced by cholesterol itself (Table 2) may reflect a compensatory mechanism due to (i) a decreased levels of Sirt1 and thus decreased deacetylation and activation of PGC-1α, which is reflected by decreased mitochondrial activity or, (ii) an effort to maintain the energetic levels of the cell. Similarly, cholesterol induced *PPAR γ* expression in Min6 cells (Table 2), which may be an attempt to restore the mitochondrial bioenergetics by supplying more substrate. Previously, PPAR γ was shown to improve substrate oxidation and increase substrate supply through increased β-fatty acid oxidation [53].

The HC diet alone also increased *PPARγ* and *LXRα* expressions in pancreas (Table 2), which is consistent with an overload of cholesterol in pancreas and an effort of the pancreas to minimize cholesterol levels. Increased *PPARγ* expression has been shown to promote cholesterol efflux through LXRα in macrophages [54] and adipocytes [55]. LXRs act as cholesterol sensors, inducing the transcription of genes that protect cells from cholesterol overload, regulating reverse cholesterol transport (RCT), cholesterol biosynthesis and cholesterol absorption/excretion [56].

4.4. Quercetin protects against the oxidative stress induced by cholesterol

We found an increase in superoxide radical levels in the mitochondria in pancreatic β-cells exposed to cholesterol (Fig. 5C). This is consistent with an incomplete reduction of oxygen to water in this organelle due to an accumulation of electron donors in the

ETC as a consequence of cholesterol-induced decrease in MMP (Fig. 4C) and OCR (Fig. 4D-H). The cholesterol-induced increase of cytosolic superoxide radicals and ROS in general (Fig. 5A,B), may be due to superoxide radical or hydrogen peroxide leakage from mitochondria through the permeability transition pore, reduced ROS scavenging, and/or increased ROS production in the cytoplasm. In fact, we found that cholesterol decreased SOD and GSH peroxidase activity in both the cytosol and mitochondria (Fig. 6). Although superoxide radicals are not strong oxidants, they are precursors of hydroxyl radicals, which possess the electrical potential necessary to initiate an oxidative chain reaction. Consistent with this, we found that cholesterol promoted lipid peroxidation (Fig. 5D) [57] which, along with a decreased GSH peroxidase activity (Fig. 6B,D,F) was also observed in the liver of cholesterol-fed rats [58].

Oxidative stress damages mtDNA impairing the ability of the organelle to replace dysfunctional electron transport proteins and decreasing bioenergetic reserve capacity; promoting ultimately mitophagic mechanisms [36]. Cholesterol by inducing oxidative stress may reduce the reserve capacity, promote mitophagy and thus induce *PGC-1α* expression, as an attempt to restore the mitochondrial mass.

Quercetin prevented the increase in the oxidant status induced by cholesterol in the β-cell line (Fig. 5). This effect may be because by its direct antioxidant properties, inherent to its chemical structure or in its indirect antioxidant properties through induction of antioxidant defences through the Nrf2 pathway and by preventing mitochondrial dysfunction (mentioned above), and its anti-inflammatory activity (discussed below). As previously reported about cholesterol [4], QUE can also activate the Nrf2 pathway, but through different mechanisms. Cholesterol promotes Nrf2 via oxidative stress since cysteine residue oxidation in Keap1 induces a conformational change that disrupts the Keap1–Nrf2 association [59], while QUE induces post-translational modifications of Nrf2 *via* the MAPK pathway [11] to allow Nrf2 translocation to the nucleus. However, we found that cholesterol inactivates antioxidant enzymes (Fig. 6), suggesting a failure to restore redox homeostasis through Nrf2 pathway. Moreover their inactivation in cytosol and in mitochondria has been reported to be ROS-mediated [60], which is consistent with QUE's protection in SOD and GSH peroxidase activities, in conjunction with its ability to prevent ROS production in both cellular compartments. Thus, we conclude that the decrease in the antioxidant defences induced by cholesterol exacerbates the oxidative status in the cell, which along with mitochondrial dysfunction (reduced reserve capacity), promotes oxidative stress.

4.5. Quercetin protects against inflammation induced by cholesterol

Our finding that cholesterol promoted NFκB activation (Fig. 7) and increased the expression of several NFκB-regulated cytokines (Table 1) indicates that NFκB activation underlies cholesterol-induced β-cell GSIS dysfunction and glycemic control impairment. The decrease in GSIS and the increase in oxidative stress and mitochondrial dysfunction in INS-1 and RINm5F pancreatic β-cells in the presence of combined cytokines: IL-1β, TNF-α and IFN-γ [20,23] suggest that cytokines exert synergic detrimental effects on insulin-secreting cells. The antioxidant properties of QUE may also contribute to the prevention of cholesterol-induced NFκB pathway activation observed in this study, since ROS are associated with NFκB activation through the increase in I-κB degradation [61].

As QUE increased *Sirt1* expression (Table 2), it is possible that QUE prevents the cholesterol-induced NFκB activation, cytokine production, and subsequent GSIS and glycemic control impairment and apoptosis observed in this study via Sirt1. It has been reported that Sirt1 inhibits the transcriptional activity of NFκB, by deacetylating the RelA/p65 subunit [62] and that overexpression of *Sirt1* in mice leads to down-regulated NFκB activity [63] and improved GSIS in β-cells [25].

The limitation of our study is that we used the whole pancreas and we did not isolate the islets of Langerhans for our biochemical studies. Thus, future studies are recommended to confirm the protective effects of QUE on pancreatic islets in *in vivo* and *ex vivo* models.

In conclusion, our study demonstrates that QUE protects against cholesterol-induced impairments in β-cell bioenergetics, thus preventing mitochondrial dysfunction and preserving insulin exocytosis and glycemic control. The improvement of ATP-linked OCR and the reserve capacity are important mechanisms of the protection of QUE against the cholesterol-induced GSIS and glycemic control impairments. Due to its antioxidant and mitochondrial protective properties QUE prevented the cholesterol-induced decrease in antioxidant defences, and the cholesterol-induced increase in cellular and mitochondrial oxidative status, thus preventing oxidative stress. The inhibition of the NFκB pathway is another important mechanism for the protection of QUE against cytokine mediated cholesterol-induced GSIS and glycemic control impairments. The deleterious effects of cholesterol were associated with a decrease in *Sirt1* expression, while QUE increase in *Sirt1* expression. This study contributes to the elucidation of the mitochondrial, cellular and molecular mechanisms underlying cholesterol-induced cytotoxicity in pancreatic β-cells, and the mitochondrial, cellular and molecular basis for the protective effects of QUE *in vitro* and *in vivo* which can contribute to improved glycemic control.

Author contributions

CC-P designed the experimental study. CC-P, KNT, STN, MR-F, NdelaJ, PLL performed the experiments. CC-P, KNT, KB and DFG-D interpreted the results. CC-P, KNT, STN and KB drafted the manuscript. All authors commented and approved the submitted manuscript.

Acknowledgments

The present study was supported by Fondecyt Initiation into Research Grant 11130232 to CC-P. We are grateful for support from IPRS and UQCent scholarships from the University of Queensland (KNT), and an MNDRIA Bill Gole Postdoctoral Research Fellowship, and The University of Queensland (STN) and NHMRC project grant (1044007, KB).

Appendix A. Supplementary material

Supplementary data associated with this article can be found in the online version at http://dx.doi.org/10.1016/j.redox.2016.08.007.

References

[1] L.R. Brunham, J.K. Kruit, T.D. Pape, J.M. Timmins, A.Q. Reuwer, Z. Vasanji, B. J. Marsh, B. Rodrigues, J.D. Johnson, J.S. Parks, C.B. Verchere, M.R. Hayden, Beta-cell ABCA1 influences insulin secretion, glucose homeostasis and response to thiazolidinedione treatment, Nat. Med. 13 (3) (2007) 340–347.

[2] I. Gerin, V.W. Dolinsky, J.G. Shackman, R.T. Kennedy, S.H. Chiang, C.F. Burant, K. R. Steffensen, J.A. Gustafsson, O.A. MacDougald, LXRbeta is required for adipocyte growth, glucose homeostasis, and beta cell function, J. Biol. Chem. 280 (24) (2005) 23024–23031.

[3] M. Hao, W.S. Head, S.C. Gunawardana, A.H. Hasty, D.W. Piston, Direct effect of cholesterol on insulin secretion: a novel mechanism for pancreatic beta-cell dysfunction, Diabetes 56 (9) (2007) 2328–2338.

[4] C. Carrasco-Pozo, M. Gotteland, R.L. Castillo, C. Chen, 3,4-dihydroxyphenylacetic acid, a microbiota-derived metabolite of quercetin, protects against pancreatic beta-cells dysfunction induced by high cholesterol, Exp. Cell Res. 4 (15) (2015) 00115–00119.

[5] M.L. Bonfleur, E.C. Vanzela, R.A. Ribeiro, G. de Gabriel Dorighello, C.P. de Franca Carvalho, C.B. Collares-Buzato, E.M. Carneiro, A.C. Boschero, H.C. de Oliveira, Primary hypercholesterolaemia impairs glucose homeostasis and insulin secretion in low-density lipoprotein receptor knockout mice independently of high-fat diet and obesity, Biochim. Biophys. Acta 1801 (2) (2010) 183–190.

[6] K. Grankvist, S.L. Marklund, I.B. Taljedal, CuZn-superoxide dismutase, Mn-superoxide dismutase, catalase and glutathione peroxidase in pancreatic islets and other tissues in the mouse, Biochem. J. 199 (2) (1981) 393–398.

[7] X. Lu, J. Liu, F. Hou, Z. Liu, X. Cao, H. Seo, B. Gao, Cholesterol induces pancreatic beta cell apoptosis through oxidative stress pathway, Cell Stress Chaperon. 16 (5) (2011) 539–548.

[8] Y.F. Zhao, L. Wang, S. Lee, Q. Sun, Y. Tuo, Y. Wang, J. Pei, C. Chen, Cholesterol induces mitochondrial dysfunction and apoptosis in mouse pancreatic beta-cell line MIN6 cells, Endocrine 37 (1) (2010) 76–82.

[9] R. Dirkx Jr, M. Solimena, Cholesterol-enriched membrane rafts and insulin secretion, J. Diabetes Investig. 3 (4) (2012) 339–346.

[10] Y. Li, I. Tabas, The inflammatory cytokine response of cholesterol-enriched macrophages is dampened by stimulated pinocytosis, J. Leukoc. Biol. 81 (2) (2007) 483–491.

[11] A.B. Granado-Serrano, M.A. Martin, L. Bravo, L. Goya, S. Ramos, Quercetin modulates Nrf2 and glutathione-related defenses in HepG2 cells: Involvement of p38, Chem. Biol. Interact. 195 (2) (2012) 154–164.

[12] M. Hamalainen, R. Nieminen, P. Vuorela, M. Heinonen, E. Moilanen, Anti-inflammatory effects of flavonoids: genistein, kaempferol, quercetin, and daidzein inhibit STAT-1 and NF-kappaB activations, whereas flavone, isorhamnetin, naringenin, and pelargonidin inhibit only NF-kappaB activation along with their inhibitory effect on iNOS expression and NO production in activated macrophages, Mediat. Inflamm. 45673 (10) (2007) 45673.

[13] G.S. Kelly, Quercetin. Monograph, Alter. Med. Rev. 16 (2) (2011) 172–194.

[14] S. Tanigawa, M. Fujii, D.X. Hou, Action of Nrf2 and Keap1 in ARE-mediated NQO1 expression by quercetin, Free Radic. Biol. Med. 42 (11) (2007) 1690–1703.

[15] C. Carrasco-Pozo, E. Pastene, C. Vergara, M. Zapata, C. Sandoval, M. Gotteland, Stimulation of cytosolic and mitochondrial calcium mobilization by indomethacin in Caco-2 cells: modulation by the polyphenols quercetin, resveratrol and rutin, Biochimica et biophysica acta 1820(12), 2012 pp. 2052–2061.

[16] M. Fiorani, A. Guidarelli, M. Blasa, C. Azzolini, M. Candiracci, E. Piatti, O. Cantoni, Mitochondria accumulate large amounts of quercetin: prevention of mitochondrial damage and release upon oxidation of the extramitochondrial fraction of the flavonoid, J. Nutr. Biochem. 21 (5) (2010) 397–404.

[17] S.S. Karuppagounder, S.K. Madathil, M. Pandey, R. Haobam, U. Rajamma, K. P. Mohanakumar, Quercetin up-regulates mitochondrial complex-I activity to protect against programmed cell death in rotenone model of Parkinson's disease in rats, Neuroscience 236 (2013) 136–148.

[18] J.M. Davis, E.A. Murphy, M.D. Carmichael, B. Davis, Quercetin increases brain and muscle mitochondrial biogenesis and exercise tolerance, Am. J. Physiol. Regul. Integr. Comp. Physiol. 296 (4) (2009) 11.

[19] T. Mandrup-Poulsen, Apoptotic signal transduction pathways in diabetes, Biochem Pharm. 66 (8) (2003) 1433–1440.

[20] X. Dai, Y. Ding, Z. Zhang, X. Cai, Y. Li, Quercetin and quercitrin protect against cytokineinduced injuries in RINm5F beta-cells via the mitochondrial pathway and NF-kappaB signaling, Int J. Mol. Med. 31 (1) (2013) 265–271.

[21] E.K. Kim, K.B. Kwon, M.Y. Song, M.J. Han, J.H. Lee, Y.R. Lee, D.G. Ryu, B.H. Park, J. W. Park, Flavonoids protect against cytokine-induced pancreatic beta-cell damage through suppression of nuclear factor kappaB activation, Pancreas 35 (4) (2007) e1–e9.

[22] W.H. Kim, J.W. Lee, B. Gao, M.H. Jung, Synergistic activation of JNK/SAPK induced by TNF-alpha and IFN-gamma: apoptosis of pancreatic beta-cells via the p53 and ROS pathway, Cell Signal. 17 (12) (2005) 1516–1532.

[23] C.Y. Lin, C.C. Ni, M.C. Yin, C.K. Lii, Flavonoids protect pancreatic beta-cells from cytokines mediated apoptosis through the activation of PI3-kinase pathway, Cytokine 59 (1) (2012) 65–71.

[24] E. Youl, G. Bardy, R. Magous, G. Cros, F. Sejalon, A. Virsolvy, S. Richard, J. F. Quignard, R. Gross, P. Petit, D. Bataille, C. Oiry, Quercetin potentiates insulin secretion and protects INS-1 pancreatic beta-cells against oxidative damage via the ERK1/2 pathway, Br. J. Pharm. 161 (4) (2010) 799–814.

[25] K.A. Moynihan, A.A. Grimm, M.M. Plueger, E. Bernal-Mizrachi, E. Ford, C. Cras-Meneur, M.A. Permutt, S. Imai, Increased dosage of mammalian Sir2 in pancreatic beta cells enhances glucose-stimulated insulin secretion in mice, Cell Metab. 2 (2) (2005) 105–117.

[26] A.G. Tabak, C. Herder, W. Rathmann, E.J. Brunner, M. Kivimaki, Prediabetes: a high-risk state for diabetes development, Lancet 379 (9833) (2012) 2279–2290.

[27] S.M. Jeong, M.J. Kang, H.N. Choi, J.H. Kim, J.I. Kim, Quercetin ameliorates hyperglycemia and dyslipidemia and improves antioxidant status in type 2 diabetic db/db mice, Nutr. Res Pract. 6 (3) (2012) 201–207.

[28] J.M. Li, W. Wang, C.Y. Fan, M.X. Wang, X. Zhang, Q.H. Hu, L.D. Kong, Quercetin preserves beta-cell mass and function in fructose-induced hyperinsulinemia through modulating pancreatic Akt/FoxO1 activation, Evid. Based Complement Altern. Med. 303902 (10) (2013) 27.

[29] N. Katsiki, E. Theocharidou, A. Karagiannis, V.G. Athyros, D.P. Mikhailidis, Ezetimibe therapy for dyslipidemia: an update, Curr. Pharm. Des. 19 (17) (2013) 3107–3114.

[30] C.-H. Lai, Y.-C. Chang, S.-Y. Du, H.-J. Wang, C.-H. Kuo, S.-H. Fang, H.-W. Fu, H.-H. Lin, A.-S. Chiang, W.-C. Wang, Cholesterol depletion reduces helicobacter pylori CagA translocation and CagA-induced responses in AGS cells, Infect. Immun. 76 (7) (2008) 3293–3303.

[31] N. Khatibzadeh, A.A. Spector, W.E. Brownell, B. Anvari, Effects of plasma membrane cholesterol level and cytoskeleton F-actin on cell protrusion mechanics, PLoS One 8(2), p. e57147.

[32] W. Ziolkowski, M. Szkatula, A. Nurczyk, T. Wakabayashi, J.J. Kaczor, R.A. Olek, N. Knap, J. Antosiewicz, M.R. Wieckowski, M. Wozniak, Methyl-beta-cyclodextrin induces mitochondrial cholesterol depletion and alters the mitochondrial structure and bioenergetics, FEBS Letters 584 (22) pp. 4606–4610.

[33] C. Carrasco-Pozo, R.L. Castillo, C. Beltrán, A. Miranda, J. Fuentes, M. Gotteland, Molecular mechanisms of gastrointestinal protection by quercetin against indomethacin-induced damage: role of NF-κB and Nrf2, J. Nutr. Biochem. 27 (2016) 289–298.

[34] M. Andriamihaja, A. Lan, M. Beaumont, M. Audebert, X. Wong, K. Yamada, Y. Yin, D. Tome, C. Carrasco-Pozo, M. Gotteland, X. Kong, F. Blachier, The deleterious metabolic and genotoxic effects of the bacterial metabolite p-cresol on colonic epithelial cells, Free Radic. Biol. Med. 85 (2015) 219–227.

[35] B.P. Dranka, G.A. Benavides, A.R. Diers, S. Giordano, B.R. Zelickson, C. Reily, L. Zou, J.C. Chatham, B.G. Hill, J. Zhang, A. Landar, V.M. Darley-Usmar, Assessing bioenergetic function in response to oxidative stress by metabolic profiling, Free Radic. Biol. Med. 51 (9) (2011) 1621–1635.

[36] B.G. Hill, G.A. Benavides, J.R. Lancaster, S. Ballinger, L. Dell'Italia, J. Zhang, V. M. Darley-Usmar, Integration of cellular bioenergetics with mitochondrial quality control and autophagy, Biol. Chem. 393 (12) (2012) 1485–1512.

[37] C. Carrasco-Pozo, K.N. Tan, K. Borges, Sulforaphane is anticonvulsant and improves mitochondrial function, J. Neurochem. 135 (5) (2015) 932–942.

[38] M.G. Hadera, O.B. Smeland, T.S. McDonald, K.N. Tan, U. Sonnewald, K. Borges, Triheptanoin partially restores levels of tricarboxylic acid cycle intermediates in the mouse pilocarpine model of epilepsy, J. Neurochem. 129 (1) (2014) 107–119, http://dx.doi.org/10.1111/jnc.12610, Epub 2013 Dec 2. (2014).

[39] E. Ulasova, J. Perez, B.G. Hill, W.E. Bradley, D.W. Garber, A. Landar, S. Barnes, J. Prasain, D.A. Parks, L.J. Dell'Italia, V.M. Darley-Usmar, Quercetin prevents left ventricular hypertrophy in the Apo E knockout mouse, Redox Biol. 1 (2013) 381–386.

[40] C. Manach, C. Morand, O. Texier, M.L. Favier, G. Agullo, C. Demigne, F. Regerat, C. Remesy, Quercetin metabolites in plasma of rats fed diets containing rutin or quercetin, J. Nutr. 125 (7) (1995) 1911–1922.

[41] M.K. Piskula, Factors affecting flavonoids absorption, Biofactors 12 (1–4) (2000) 175–180.

[42] M.D. Brand, D.G. Nicholls, Assessing mitochondrial dysfunction in cells, Biochem. J. 435 (2) (2011) 297–312.

[43] V. Giorgio, S. von Stockum, M. Antoniel, A. Fabbro, F. Fogolari, M. Forte, G. D. Glick, V. Petronilli, M. Zoratti, I. Szabo, G. Lippe, P. Bernardi, Dimers of mitochondrial ATP synthase form the permeability transition pore, Proc. Natl. Acad. Sci. USA 110 (15) (2013) 5887–5892.

[44] E. Latz, T.S. Xiao, A. Stutz, Activation and regulation of the inflammasomes, Nat. Rev. Immunol. 13 (6) (2013) 397–411.

[45] S.C. Lim, K.R. Parajuli, H.Q. Duong, J.E. Choi, S.I. Han, Cholesterol induces autophagic and apoptotic death in gastric carcinoma cells, Int J. Oncol. 44 (3) (2014) 805–811.

[46] H. Vaziri, S.K. Dessain, E. Ng Eaton, S.I. Imai, R.A. Frye, T.K. Pandita, L. Guarente, R.A. Weinberg, hSIR2(SIRT1) functions as an NAD-dependent p53 deacetylase, Cell 107 (2) (2001) 149–159.

[47] H.Y. Cohen, S. Lavu, K.J. Bitterman, B. Hekking, T.A. Imahiyerobo, C. Miller, R. Frye, H. Ploegh, B.M. Kessler, D.A. Sinclair, Acetylation of the C terminus of Ku70 by CBP and PCAF controls Bax-mediated apoptosis, Mol. Cell 13 (5) (2004) 627–638.

[48] J.C. Hou, L. Min, J.E. Pessin, Insulin granule biogenesis, trafficking and exocytosis, Vitam. Horm. 80 (2009) 473–506.

[49] J.S. Bogan, Y. Xu, M. Hao, Cholesterol accumulation increases insulin granule size and impairs membrane trafficking, Traffic 13 (11) (2012) 1466–1480.

[50] C. Reily, T. Mitchell, B.K. Chacko, G. Benavides, M.P. Murphy, V. Darley-Usmar, Mitochondrially targeted compounds and their impact on cellular bioenergetics, Redox Biol. 1 (1) (2013) 86–93.

[51] P.J. Fernandez-Marcos, J. Auwerx, Regulation of PGC-1α, a nodal regulator of mitochondrial biogenesis, Am. J. Clin. Nutr. 93 (4) (2011) 884S–890S.

[52] R. Ventura-Clapier, A. Garnier, V. Veksler, Transcriptional control of mitochondrial biogenesis: the central role of PGC-1alpha, Cardiovasc Res. 79 (2) (2008) 208–217.

[53] F.A. Monsalve, R.D. Pyarasani, F. Delgado-Lopez, R. Moore-Carrasco, Peroxisome proliferator-activated receptor targets for the treatment of metabolic diseases, Mediat. Inflamm. 2013 (2013) 549627, http://dx.doi.org/10.1155/2013/549627, Epub 2013 May 27. (2013).

[54] A.D. Baker, A. Malur, B.P. Barna, M.S. Kavuru, A.G. Malur, M.J. Thomassen, PPARγ regulates the expression of cholesterol metabolism genes in alveolar macrophages, Biochem. Biophys. Res. Commun. 393 (4) (2010) 682–687.

[55] S.Z. Dong, S.P. Zhao, Z.H. Wu, J. Yang, X.Z. Xie, B.L. Yu, S. Nie, Curcumin promotes cholesterol efflux from adipocytes related to PPARgamma-LXRalpha-ABCA1 passway, Mol. Cell Biochem. 358 (1–2) (2011) 281–285.

[56] C. Zhao, K. Dahlman-Wright, Liver X receptor in cholesterol metabolism, J. Endocrinol. 204 (3) (2010) 233–240.
[57] J.M. Gutteridge, D.A. Rowley, B. Halliwell, Superoxide-dependent formation of hydroxyl radicals and lipid peroxidation in the presence of iron salts. Detection of 'catalytic' iron and anti-oxidant activity in extracellular fluids, Biochem. J. 206 (3) (1982) 605–609.
[58] A.C. Tsai, Lipid peroxidation and glutathione peroxidase activity in the liver of cholesterol-fed rats, J. Nutr. 105 (7) (1975) 946–951.
[59] H.K. Bryan, A. Olayanju, C.E. Goldring, B.K. Park, The Nrf2 cell defence pathway: Keap1-dependent and -independent mechanisms of regulation, Biochem. Pharm. 85 (6) (2013) 705–717.
[60] E. Pigeolet, J. Remacle, Susceptibility of glutathione peroxidase to proteolysis after oxidative alteration by peroxides and hydroxyl radicals, Free Radic. Biol. Med 11 (2) (1991) 191–195.
[61] N. Li, M. Karin, Is NF-kappaB the sensor of oxidative stress? FASEB J.: Off. Publ. Fed. Am. Soc. Exp. Biol. 13 (10) (1999) 1137–1143.
[62] F. Yeung, J.E. Hoberg, C.S. Ramsey, M.D. Keller, D.R. Jones, R.A. Frye, M.W. Mayo, Modulation of NF-κB-dependent transcription and cell survival by the SIRT1 deacetylase, EMBO J. 23 (12) (2004) 2369–2380.
[63] P.T. Pfluger, D. Herranz, S. Velasco-Miguel, M. Serrano, M.H. Tschop, Sirt1 protects against high-fat diet-induced metabolic damage, Proc. Natl. Acad. Sci. USA 105 (28) (2008) 9793–9798.
[64] H.K. Bryan, A. Olayanju, C.E. Goldring, B.K. Park, The Nrf2 cell defence pathway: Keap1-dependent and -independent mechanisms of regulation, Biochem. Pharm. 85 (6) (2013) 705–717.
[65] E. Pigeolet, J. Remacle, Susceptibility of glutathione peroxidase to proteolysis after oxidative alteration by peroxides and hydroxyl radicals, Free Radic. Biol. Med 11 (2) (1991) 191–195.
[66] N. Li, M. Karin, Is NF-kappaB the sensor of oxidative stress? FASEB J.: Off. Publ. Fed. Am. Soc. Exp. Biol. 13 (10) (1999) 1137–1143.
[67] F. Yeung, J.E. Hoberg, C.S. Ramsey, M.D. Keller, D.R. Jones, R.A. Frye, M.W. Mayo, Modulation of NF-κB-dependent transcription and cell survival by the SIRT1 deacetylase, EMBO J. 23 (12) (2004) 2369–2380.
[68] P.T. Pfluger, D. Herranz, S. Velasco-Miguel, M. Serrano, M.H. Tschop, Sirt1 protects against high-fat diet-induced metabolic damage, Proc. Natl. Acad. Sci. USA 105 (28) (2008) 9793–9798.